

## Channel Function Is Dissociated from the Intrinsic Kinase Activity and Autophosphorylation of TRPM7/ChaK1\*

Received for publication, December 6, 2004, and in revised form, February 22, 2005  
Published, JBC Papers in Press, March 21, 2005, DOI 10.1074/jbc.M413671200

Masayuki Matsushita<sup>‡</sup>, J. Ashot Kozak<sup>§¶</sup>, Yoshio Shimizu<sup>||</sup>, Derek T. McLachlin<sup>\*\*‡‡</sup>,  
Hiroto Yamaguchi<sup>§§</sup>, Fan-Yan Wei<sup>‡</sup>, Kazuhito Tomizawa<sup>‡</sup>, Hideki Matsui<sup>‡</sup>, Brian T. Chait<sup>\*\*</sup>,  
Michael D. Cahalan<sup>§</sup>, and Angus C. Nairn<sup>¶¶|||</sup>

From the <sup>‡</sup>First Department of Physiology, Okayama University Medical School, 2-5-1 Shikata-cho, Okayama 700-8558, Japan, the <sup>§§</sup>Department of Structure Biology, Nara Institute of Science and Technology, 8916-5 Takayama, Ikoma Nara 630-0101, Japan, <sup>||</sup>Laboratory of Molecular and Cellular Neuroscience and <sup>\*\*</sup>Laboratory of Mass Spectrometry, The Rockefeller University, New York, New York 10021, the <sup>§</sup>Department of Physiology and Biophysics, University of California, Irvine, California 92697-4561, and the <sup>¶¶</sup>Department of Psychiatry, Yale University School of Medicine, New Haven, Connecticut 06508

TRPM7/ChaK1 is a unique channel/kinase that contains a TRPM channel domain with 6 transmembrane segments fused to a novel serine-threonine kinase domain at its C terminus. The goal of this study was to investigate a possible role of kinase activity and autophosphorylation in regulation of channel activity of TRPM7/ChaK1. Residues essential for kinase activity were identified by site-directed mutagenesis. Two major sites of autophosphorylation were identified *in vitro* by mass spectrometry at Ser<sup>1511</sup> and Ser<sup>1567</sup>, and these sites were found to be phosphorylated in intact cells. TRPM7/ChaK1 is a cation-selective channel that exhibits strong outward rectification and inhibition by millimolar levels of internal [Mg<sup>2+</sup>]. Mutation of the two autophosphorylation sites or of a key catalytic site that abolished kinase activity did not alter channel activity measured by whole-cell recording or Ca<sup>2+</sup> influx. Inhibition by internal Mg<sup>2+</sup> was also unaffected in the autophosphorylation site or “kinase-dead” mutants. Moreover, kinase activity was enhanced by Mg<sup>2+</sup>, was decreased by Zn<sup>2+</sup>, and was unaffected by Ca<sup>2+</sup>. In contrast, channel activity was inhibited by all three of these divalent cations. However, deletion of much of C-terminal kinase domain resulted in expression of an apparently inactive channel. We conclude that neither current activity nor regulation by internal Mg<sup>2+</sup> is affected by kinase activity or autophosphorylation but that the kinase domain may play a structural role in channel assembly or subcellular localization.

Recent studies have characterized several unique protein kinases that display no amino acid sequence similarity to the superfamily of protein kinase A-related enzymes, including

\* This work was supported by United States Public Health Service Grants GM50402 (to A. C. N.), NS14609 (to M. D. C.), and RR00862 (to B. T. C.) and by a grant-in-aid from the Ministry of Education, Science, Sports, and Culture of Japan (to M. M.). The costs of publication of this article were defrayed in part by the payment of page charges. This article must therefore be hereby marked “advertisement” in accordance with 18 U.S.C. Section 1734 solely to indicate this fact.

¶ Recipient of an American Heart Association Postdoctoral Fellowship.

‡‡ Recipient of a postdoctoral fellowship from the Canadian Institutes of Health Research.

||| To whom correspondence should be addressed: Dept. of Psychiatry, Yale University School of Medicine, New Haven, CT 06508. Tel.: 203-974-7725; Fax: 203-974-7724; E-mail: angus.nairn@yale.edu.

eukaryotic elongation factor-2 kinase (EF2K)<sup>1</sup> and *Dictyostelium* myosin heavy chain kinases A, B, and C (MHCK A–C). Several additional catalytic domains related to EF2K and MHCK have been identified through data base searches in mammals as well as in nematode worm, although the function of these potential protein kinases is not known (1–3). Using this approach, we and others identified an 1863-amino acid polypeptide (termed ChaK for channel kinase) that contained a TRP-related channel domain fused to the atypical kinase domain at its C terminus (3, 4). The same gene product was also identified in a yeast two-hybrid screen using a portion of phospholipase C  $\beta$ 1 as bait (and termed TRP-PLIK) (5) and in a screen for TRP-related channels (and termed LTRPC7) (6). Based on revised nomenclature for TRP channels, the kinase-containing TRP has been termed TRPM7/ChaK1 based on its similarity to long TRP family members, melastatin, MTR1 (TRPM5), and LTRPC2 (TRPM2) (7). A closely related gene, TRPM6/ChaK2 has also been identified as being mutated in familial hypomagnesemia (8, 9), and a key role for both TRPM6 and TRPM7 has been suggested in Mg<sup>2+</sup> homeostasis (8–11).

Members of the TRP family of channels contain six predicted transmembrane segments and are related to the superfamily of ion channels that include voltage-gated K<sup>+</sup> channels and cyclic nucleotide-gated channels (12, 13). In addition to the kinase domain at the C terminus of TRPM7, other regions of potential functional importance are a putative coiled-coil domain and a domain enriched in Ser/Pro and Thr/Pro motifs (the STP domain) (Fig. 1A). We have recently determined the crystal structure of the kinase domain of TRPM7 (4). The TRPM7 kinase domain (residues 1551–1577) forms a domain-swapped bilobate dimer. Despite a lack of amino acid sequence similarity to the classical eukaryotic protein kinases, the TRPM7 kinase domain exhibits within its N-terminal lobe secondary and tertiary structural similarity to the protein kinase A superfamily as well as to metabolic enzymes with ATP grasp domains. However, in contrast to the classical kinase superfamily, the C-terminal lobe of the TRPM7 kinase domain contains a zinc finger homology domain, and zinc appears to play a structural role in TRPM7 and related EF2K/MHCK family members (4).

Previous studies in heterologous expression systems have

<sup>1</sup> The abbreviations used are: EF2K, eukaryotic elongation factor-2 kinase; MHCK, myosin heavy chain kinase; MBP, myelin basic protein; MALDI, matrix-assisted laser desorption/ionization; TOF, time-of-flight; HPLC, high pressure liquid chromatography; MS, mass spectrometry; GST, glutathione S-transferase; GFP, green fluorescent protein; CHO, Chinese hamster ovary.

indicated that TRPM7 exhibits a steep outwardly rectifying current-voltage relation and permeability to monovalent and divalent cations (5, 6). Nadler *et al.* (6) demonstrated that millimolar concentrations of internal  $Mg^{2+}$ , MgATP, MgGTP, or other  $Mg^{2+}$ -nucleotides inhibit TRPM7. In RBL and Jurkat T cells, the native correlate of TRPM7 was described and termed MagNuM (magnesium nucleotide-dependent metal cation) (14), or MIC ( $Mg^{2+}$ -inhibited cation) (15, 16). Similar currents have also been described in cardiac fibroblasts (17), smooth muscle cells (18), and brain microglia (19).

The role of the kinase domain and phosphorylation in the ion channel function is controversial (for a recent review, see Ref. 20). Runnels *et al.* (5) reported that mutations of kinase domain residues (probably involved in ATP and zinc binding (4)) apparently abolished channel activity measured in whole-cell recording. Subsequently, Schmitz *et al.* (10) showed that whereas TRPM7 mutants with impaired kinase activity formed functional channels, these channels exhibited reduced sensitivity to  $Mg^{2+}$ . Moreover, a kinase deletion mutant exhibited increased  $Mg^{2+}$  sensitivity. From these studies, Schmitz *et al.* (10) concluded that the TRPM7 kinase domain was somehow coupled negatively to the mechanism(s) that mediated  $Mg^{2+}$ -dependent inhibition.

In this study, we have characterized the biochemical and functional properties of the TRPM7 kinase activity. Guided by the crystal structure, we have confirmed the identity of amino acids critical for kinase activity. We have identified two major sites of TRPM7 autophosphorylation by mass spectrometry and demonstrated that these sites are phosphorylated in intact cells. Using whole-cell patch clamp recording, we have measured the magnitude of the constitutive current conducted by wild-type TRPM7 and its kinase-dead and autophosphorylation site variants and compared the extent of inhibition by internal  $Mg^{2+}$  among them. We have also measured the corresponding  $Ca^{2+}$  influx in intact mammalian cells overexpressing the wild-type channel and the variants. We show that autophosphorylation site or kinase-dead TRPM7 mutant channels do not differ from wild-type channels in their ability to form functional ion channels and in their sensitivity to internal  $Mg^{2+}$ . Thus, TRPM7 channel function and regulation by  $Mg^{2+}$  are clearly dissociated from autophosphorylation or kinase activity. Interestingly, results obtained following deletion of the much of the kinase domain suggest that this C-terminal region may play a structural role in channel assembly or subcellular localization.

#### EXPERIMENTAL PROCEDURES

**cDNA Cloning**—Data base analysis, which used tBlastN, identified the expressed sequence tag, AA138771 (GenBank<sup>TM</sup>). Mouse embryo rapid screen cDNA library panels (OriGene Technologies, Rockville, MD) were screened by PCR using the primers based on the expressed sequence tag sequence (sense, 5'-AGCAGTCAAAGTGCTGTGTAC-3'; antisense, 5'-CATCTCTCCTAGATTGGCAG-3'). A mouse embryo library (Clontech, Palo Alto, CA) was then screened using a fragment from the PCR analysis. Multiple rounds of screening subsequently yielded 50 independent overlapping cDNA clones, which were sequenced and aligned. For expression in mammalian cells, full-length TRPM7, TRPM7- $\Delta$ KD, and TRPM7 mutants were cloned into the pcDNA3.1 vector (Invitrogen).

**Expression of Wild-type and Mutant TRPM7 Kinase Domain in Sf9 Cells**—A recombinant 316-residue kinase domain fragment (TRPM7 residues 1548–1863) was expressed in Sf9 insect cells with a hexahistidine tag by using the Bac-to-Bac baculovirus expression system (Invitrogen) essentially as described (4). The expressed protein was purified using Q-Sepharose (Amersham Biosciences) and  $Ni^{2+}$ -nitrilotriacetic acid Superflow (Qiagen, Hilden, Germany). A PCR-based site-directed mutagenesis method was employed to generate point mutants, R1622L, K1646R, K1727A, N1731V, D1765N, D1765A, Q1767N, Q1767A, T1774S, T1774A, D1775A, and N1795A. The wild type pFastBac construct was used as a template, and PCR was carried

out for each mutant with a set of sense and antisense mutagenic primers (essentially as described in the Stratagene QuikChange<sup>TM</sup> kit). The PCR products were treated with DpnI restriction enzyme and purified through agarose gel electrophoresis. Purified DNA was used to transform *Escherichia coli* (DH5a), and transformants harboring mutant constructs were identified. Mutations were confirmed by DNA sequencing. Mutant pFastBac constructs were used to generate mutant recombinant viruses, and protein was expressed and purified as in the case of wild type.

**Expression of GST-TRPM7 Kinase Domain in E. coli**—For bacterial expression, DNA fragments were subcloned in frame with GST using the pGEX-4T-2 vector (Amersham Biosciences). GST fusion proteins including either residues 1180–1863 or 1580–1863 of TRPM7 were expressed in *E. coli* (DE3) and purified using standard methods.

**Phosphorylation Assays**—Reaction mixtures (100  $\mu$ l) contained 50 mM HEPES (pH 7.5), 10 mM magnesium acetate (unless otherwise indicated), 5 mM dithiothreitol, 100  $\mu$ M [<sup>32</sup>P]ATP (specific activity, 2–5  $\times$  10<sup>2</sup> cpm/pmol), and GST-TRPM7-KD (10  $\mu$ g/ml) or Sf9 cell TRPM7-KD or mutant proteins (~1  $\mu$ g/ml), with or without myelin basic protein (MBP; 50  $\mu$ g/ml). For analysis of the effect of  $Mg^{2+}$  and other divalent cations on kinase activity, GST-TRPM7 was incubated with MBP in a reaction mixture containing different concentrations of  $Mg^{2+}$ ,  $Ca^{2+}$ , and  $Zn^{2+}$ . All reactions were initiated by the addition of [<sup>32</sup>P]ATP and carried out at 30 °C for 10–30 min. In the studies shown in Figs. 3D and 4B, GST-TRPM7-(1180–1863) (wild-type sequence), GST-TRPM7-(1180–1863) (S1511A and S1567A; see details below), and GST-TRPM7-(1180–1863) (TAP sequence; see details below) (100 ng/ml) were incubated in 50 mM Tris-HCl, pH 7.4, 10 mM  $MgCl_2$ , 20 mM EGTA, 1 mM dithiothreitol, 100  $\mu$ M ATP for 30 min at 30 °C (in Fig. 3D, [<sup>32</sup>P]ATP was also included). Reactions were terminated by the addition of SDS sample buffer, and samples were analyzed by SDS-PAGE (10% polyacrylamide). Gels were stained with Coomassie Brilliant Blue, destained, dried and subjected to autoradiography or analysis using a phosphor imager (Fuji). Phosphoamino acid analysis and two-dimensional peptide mapping were performed as described (21).

**Phosphorylation in Intact Cells**—HEK293 cells were transfected with wild-type TRPM7 using FuGENE 6 (Roche Applied Science). Wild-type TRPM7 was expressed for 24–48 h, and cells were labeled with <sup>32</sup>P<sub>i</sub> for 2 h. Cells were incubated without or with ionomycin (5  $\mu$ M) for 5 min, cell lysates were prepared, and TRPM7 was immunoprecipitated with anti-FLAG M2 affinity gel (Sigma). Samples were analyzed by SDS-PAGE and autoradiography. In other studies, HEK293 cells were transfected with wild-type TRPM7 or TRPM7-TAP using Lipofectamine 2000 (Invitrogen). Cell lysates were prepared, and TRPM7 was immunoprecipitated with anti-FLAG M2 affinity gel. Samples were analyzed by SDS-PAGE and immunoblotted using phospho-specific or FLAG antibodies.

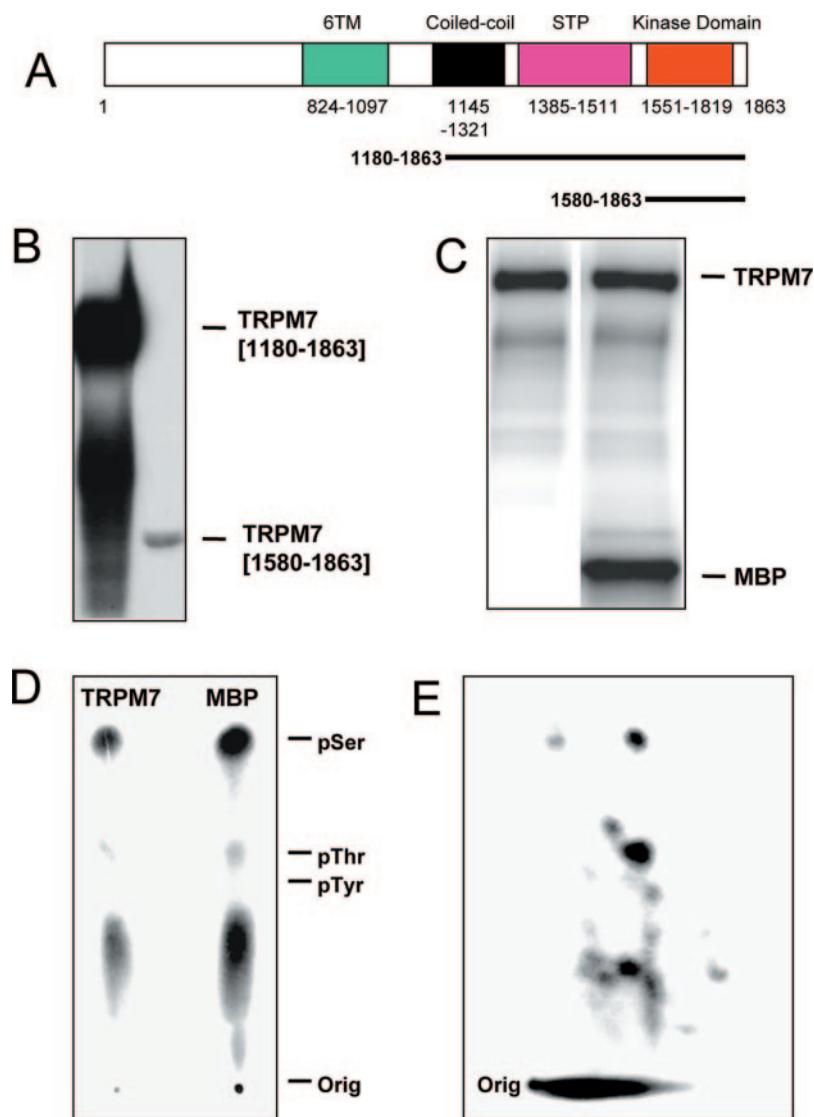
**Mass Spectrometry**—After SDS-PAGE, bands containing autophosphorylated TRPM7 were excised from the gel, destained, and digested with trypsin (Roche Applied Science). The tryptic peptides were eluted from the gel and collected on POROS R2 beads (Applied Biosystems, Foster City, CA). After washing, the peptides were eluted from the beads and spotted onto a matrix-assisted laser desorption/ionization (MALDI) target using 2,5-dihydrobenzoic acid (Sigma) as matrix. MALDI time-of-flight (TOF) mass spectrometry was carried out on a Voyager-DE STR instrument (Applied Biosystems, Foster City, CA). MALDI-ion trap analysis was performed on a modified LCQ (Thermo Finnegan, San Jose, CA) mass spectrometer (22). On-line HPLC-MS/MS was performed using a 0.2  $\times$  50-mm MAGIC MS C18 column (Michrom Bioresources, Auburn, CA) connected directly to an LCQ-DECA electrospray-ion trap mass spectrometer (Thermo Finnegan).

**Immunofluorescence and Immunoblotting**—Antibodies to TRPM7 were made against GST fusion proteins that contained the coiled-coil domain (residues 1145–1321) (in rabbit) or the kinase domain (residues 1580–1863) (in guinea pig) of TRPM7. A phosphorylation state-specific antibody that specifically recognizes phospho-Ser<sup>1567</sup> of TRPM7 was generated in rabbit using as antigen a phosphopeptide corresponding to residues 1562–1571 of mouse TRPM7. Antibodies were affinity-purified by absorption to immobilized recombinant proteins or phosphopeptide. For indirect immunofluorescence using confocal microscopy, HEK293 cells were fixed with 4% formaldehyde in PBS and permeabilized in 0.1% Triton X-100 (in PBS). After blocking (5% milk powder) for 30 min, cells were incubated with anti-TRPM7 antibody (guinea pig) for 2 h, washed three times in washing buffer, and incubated with fluorescein isothiocyanate-conjugated anti-guinea pig antibody for 30 min. Immunoblotting was carried out using standard procedures, and proteins were identified by ECL (Amersham Biosciences).

**Ca<sup>2+</sup> Imaging of HEK293 Cells**—HEK293 cells (RIKEN, Tsukuba,

### FIG. 1. Ser/Thr protein kinase activity and autophosphorylation of TRPM7.

**A**, the diagram shows the domain organization of TRPM7, including the six transmembrane-spanning helices that define the TRP-like channel (green), a putative coiled-coil domain (black), a region rich in serine, threonine, and proline residues (STP; pink), and the EF2/MHCK-like kinase domain (red). The black bars indicate two of the protein fragments expressed in *E. coli* as GST fusion proteins. **B**, autophosphorylation of GST-TRPM7-(1580–1863) (right) and GST-TRPM7-(1180–1863) (left). GST-TRPM7 kinase domains were incubated with [<sup>32</sup>P]ATP for 30 min. Samples were separated by SDS-PAGE and analyzed by autoradiography. **C**, TRPM7-(1180–1863) was incubated alone (left lane) or with MBP (right lane) and [<sup>32</sup>P]ATP for 10 min. Samples were separated by SDS-PAGE and analyzed by autoradiography. **D**, phosphoamino acid analysis of autophosphorylated GST-TRPM7-(1180–1863) and MBP. Aliquots of tryptic digests were hydrolyzed with HCl, and phosphoamino acids were separated by electrophoresis. [<sup>32</sup>P]phosphoamino acids were visualized by autoradiography, and the positions of phosphotyrosine (pY), phosphothreonine (pT), and phosphoserine (pS) standards are indicated. The radioactive material between the origin and phosphotyrosine is unhydrolyzed peptide. **E**, two-dimensional tryptic phosphopeptide map of autophosphorylated TRPM7-(1180–1863). The sample was separated by electrophoresis in the first dimension (origin left, positive right) and by ascending chromatography in the second dimension. Major phosphopeptides a, b, and c are indicated. The radioactive material at the origin probably represents undigested protein.



Japan) were transfected with wild-type TRPM7 and various mutants using Lipofectamine 2000 reagent (Invitrogen). Transfection efficiencies, estimated by immunofluorescence staining, were typically >80%. Transfected cells were washed in HEPES-buffered saline (120 mM NaCl, 5.3 mM KCl, 0.8 mM MgSO<sub>4</sub>, 1.8 mM CaCl<sub>2</sub>, 11.1 mM glucose, 20 mM HEPES-Na (pH 7.4)) and loaded with 5 μM FURA-2/AM (Molecular Probes, Inc., Eugene, OR) for 1 h at room temperature. Cells were then incubated in HEPES-buffered saline for 20 min at 37 °C to allow cleavage of the acetoxymethyl ester. Fluorescence images of the cells were recorded at room temperature and analyzed with a video image analysis system (AquaCosmos; Hamamatsu Photonics, Hamamatsu, Japan), with excitation alternatively at 340 and 380 nm and emission at 510 nm. Data from 30–50 individual cells were collected per experiment, and ensemble averages were calculated from multiple experiments. Data acquisition was typically for 5-s intervals and lasted for 15 min.

**Electrophysiology**—CHO-K1 cells were grown in F-12K medium with L-glutamine (ATCC, Manassas, VA) supplemented with 10% fetal bovine serum (Omega Scientific, Tarzana, CA). Cells were grown in 6-well polystyrene dishes, and 1 day after plating they were transfected using Effectene (Qiagen) according to the manufacturer's protocol. The TRPM7 plasmid (pcDNA3.1) DNA was supplemented with enhanced GFP plasmid (eGFPN3; Clontech) at a 5:1 ratio in order to visualize the transfected cells by their enhanced GFP fluorescence (23). Transfection continued for ~12 h. For mock transfection, the same procedure was employed, except DNA was omitted. Cells were subsequently trypsinized and plated on acid-washed glass coverslips for recording. For whole-cell patch clamp recording, coverslips with CHO cells were placed on a stage of an inverted microscope (Zeiss IM-35) and superfused with the external solution used for recording. GFP-positive cells

were visualized using mercury arc lamp illumination at 290-nm wavelength. Recombinant TRPM7 channel currents were recorded in the whole-cell patch clamp using an EPC-9 patch clamp amplifier (HEKA Elektronik, Lambrecht, Germany). Command voltage ramps from –110 to +85 mV (211-ms duration) were applied at 0.5-Hz frequency, and the resulting currents were digitized at 200 μs. Cell and electrode capacitance was compensated with the EPC-9 circuitry. Series resistance was compensated by 85% to avoid potential errors due to large current amplitudes. Resistances of the fire-polished pipettes measured with the internal solutions were 1.5–4 megaohms. The silver-silver chloride ground electrode was connected to the bath solution via an agar bridge. All recordings were made at room temperature. The current amplitude was measured at +80 mV and plotted against time after whole cell recording mode was established. In the majority of cells, the current had reached its maximum less than 6 min after break-in. All CHO cells tested exhibited an endogenous MIC current thought to represent native TRPM7 channels. The endogenous MIC current amplitude at +80 mV averaged 30.6 pA/picofarad (S.E. = 5.6, n = 12). Igor Pro (WaveMetrics, Lake Oswego, OR) and Microcal Origin (Microcal Software, Northampton, MA) were used to analyze the data.

The following internal solutions were used to record from CHO cells overexpressing wild-type TRPM7 and mutants. The 0 Mg<sup>2+</sup> solution contained 130 mM Cs<sup>+</sup> glutamate, 12 mM EGTA, 0.9 mM CaCl<sub>2</sub>, 10 mM HEPES, pH 7.3. The 4 and 6.5 mM Mg<sup>2+</sup> solutions had 130 mM Cs<sup>+</sup> glutamate, 12 mM EGTA, 0.9 mM CaCl<sub>2</sub>, 4 mM/6.5 mM MgCl<sub>2</sub>, 10 mM HEPES, pH 7.3. The free Mg<sup>2+</sup> concentrations in these solutions were 2.3 and 4 mM, respectively, as calculated by Maxchelator software. The external solution contained 4.5 mM K, 162 mM Na<sup>+</sup> aspartate, 2 mM CaCl<sub>2</sub>, 10 mM HEPES, 2 mM glucose, pH 7.3. For testing Ca<sup>2+</sup> and Zn<sup>2+</sup>

inhibition of TRPM7 current, EGTA in the internal solution was replaced with 1 mM EDTA and 5 mM CaCl<sub>2</sub> or ZnCl<sub>2</sub> added as indicated. Salts were purchased from Sigma and Calbiochem.

## RESULTS

**Characterization of the Kinase Activity and Autophosphorylation of TRPM7**—To examine the kinase activity of TRPM7, several GST fusion proteins containing the kinase domain and additional N-terminal extensions were expressed in *E. coli* and purified (Fig. 1 and data not shown). A high level of autophosphorylation of TRPM7-(1180–1863) was observed, predominantly on serine with low phosphorylation of threonine (Fig. 1, *B* and *D*). In contrast, much lower autophosphorylation was found for a fragment that contained just the kinase domain (TRPM7-(1580–1863)) (Fig. 1*B*). Two-dimensional tryptic peptide mapping revealed multiple phosphopeptides (Fig. 1*E*). TRPM7 also phosphorylated the exogenous substrate, myelin basic protein (MBP), largely on serine residues with low phosphorylation on threonine residues (Fig. 1, *C* and *D*).

We recently determined the crystal structure of the kinase domain of TRPM7 (4). Whereas the likely function of several key amino acids in the kinase domain of TRPM7 was implied by analogy with residues in the classical kinase superfamily, it was important to directly analyze the properties of these residues using site-directed mutagenesis. Moreover, the availability of mutant (kinase-dead) TRPM7 was necessary for the studies described below. Mutation of residues (Arg<sup>1622</sup> to leucine; Lys<sup>1727</sup> to alanine; Asn<sup>1731</sup> to valine; Thr<sup>1774</sup> to serine or alanine) likely to be involved directly in binding of phosphate groups of ATP or residues (Gln<sup>1767</sup> to asparagine or alanine; Asp<sup>1775</sup> to alanine) likely to be involved in metal binding all resulted in very low activity (Fig. 2, *A* and *B*). Similarly, mutation of residues implicated in catalysis (Lys<sup>1646</sup> to arginine; equivalent to the conserved lysine residue of classical kinases that is often mutated to produce a kinase-dead protein; Asp<sup>1765</sup> to asparagine or alanine) resulted in very low activity. Mutation of a residue in the glycine motif (Asn<sup>1795</sup> to alanine) that may be involved in peptide substrate binding or orientation of the substrate-binding loop resulted in low but measurable activity.

**Mass Spectrometric Analysis of Phosphorylation Sites in TRPM7**—TRPM7-(1180–1863) phosphorylated *in vitro* as described above was subjected to SDS-PAGE. The TRPM7 band was digested in the gel with trypsin, and the tryptic peptides were analyzed by MALDI-TOF mass spectrometry (Fig. 3*A*). Since the addition of HPO<sub>3</sub> causes an increase in mass of 80 Da, potential phosphopeptides within the tryptic map were identified by searching the observed signals for shifts of 80 Da relative to expected tryptic peptides. Three peptides showing an 80-Da shift were observed, corresponding to residues 1564–1576 (predicted phosphorylated mass 1516.7 Da, observed mass 1516.4 Da), 1501–1521 (predicted mass 2380.5, observed mass 2380.3), and 1564–1584 (predicted mass 2418.7, observed mass 2418.4). These peptides were subjected to fragmentation in a MALDI-ion trap mass spectrometer (22); each one showed a facile loss of 98 Da due to elimination of the elements of H<sub>3</sub>PO<sub>4</sub>, confirming that each was phosphorylated. Other fragment ions confirmed the identity of each tryptic peptide. The MS<sup>2</sup> spectrum of the 1501–1521 peptide contained fragment ions showing that the major site of phosphorylation in this peptide was Ser<sup>1511</sup> (data not shown). The MALDI-ion trap fragmentation data from the other two peptides did not allow us to determine whether Ser<sup>1565</sup> or Ser<sup>1567</sup> was the site of phosphorylation, so the 1564–1584 peptide was analyzed by HPLC-MS/MS (Fig. 3, *B* and *C*). The fragmentation pattern of the triply charged ion indicated that Ser<sup>1567</sup> was phosphorylated in the 1564–1584 peptide.

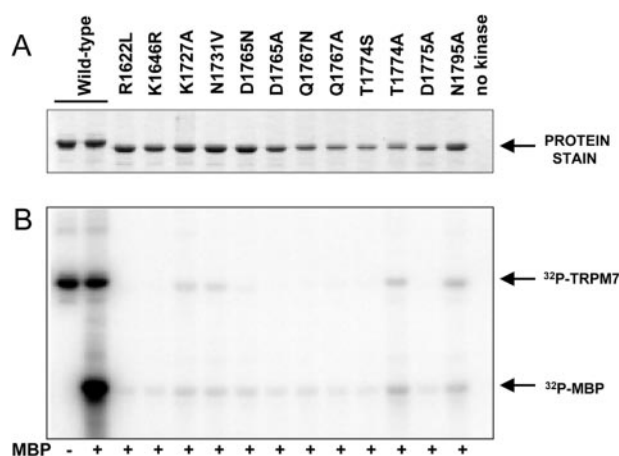


**FIG. 2. Characterization of the kinase activity of TRPM7 kinase.** *A*, TRPM7-(1548–1863) and various site-directed mutants (as indicated) were expressed in Sf9 cells using the baculovirus method. Proteins were purified and analyzed by SDS-PAGE and staining with Coomassie Blue. *B*, wild-type and mutant kinase domains were incubated with [<sup>32</sup>P]ATP and MBP (as indicated) for 10 min using standard assay conditions. Samples were separated by SDS-PAGE and analyzed by autoradiography. The far left lane shows autophosphorylation of wild-type TRPM7-(1548–1863) in the absence of MBP. Analysis of the phosphorylation of MBP using a phosphor imager indicated that (after taking into account the slight differences in the levels of protein for the TRPM7 kinase mutants), the various kinase mutants exhibited <1% of the activity of the wild-type kinase, except for TRPM7-T1774A (~6% of wild-type) and TRPM7-N1795A (~2% of wild-type). For comparison, the specific activity (using MBP as substrate) of wild-type GST-TRPM7-(1180–1863) was 50.1 pmol/min/μg, whereas that of GST-TRPM7-(1180–1863), containing the D1775A mutation, was 0.1 pmol/min/μg (0.2% of wild type). Under the same conditions, ERK phosphorylated MBP with a specific activity of 486 pmol/min/μg.

Mutation of both Ser<sup>1511</sup> and Ser<sup>1567</sup> to alanine resulted in a large decrease in autophosphorylation compared with wild-type GST-TRPM7-(1180–1863), indicating that Ser<sup>1511</sup> and Ser<sup>1567</sup> represent major sites of phosphorylation (Fig. 3*D*). To further confirm Ser<sup>1567</sup> as a major *in vitro* autophosphorylation site, we prepared a phospho-specific antibody that recognized wild-type TRPM7 autophosphorylated *in vitro* (Fig. 4*B*). However, the phospho-Ser<sup>1567</sup> antibody did not detect any signal in a mutant (TRPM7-TAP) in which the kinase activity was inactivated by substitution of the key catalytic residue in the conserved “TDP” motif found in EF2K/MHCK family members (TRPM7-D1775A; see Fig. 2).

**Phosphorylation of TRPM7 in Intact Cells**—To investigate whether Ser<sup>1511</sup> and/or Ser<sup>1567</sup> were phosphorylated in intact cells, wild-type TRPM7 was expressed in HEK293 cells, cells were labeled with <sup>32</sup>Pi, and the phosphorylation of TRPM7 analyzed following immunoprecipitation (Fig. 4*A*). In control conditions, TRPM7 was strongly labeled with phosphorylation occurring almost exclusively on serine residues (Fig. 4*E*). Comparison of the phosphopeptide tryptic map of full-length TRPM7 phosphorylated in HEK293 cells (Fig. 4*C*) with that of TRPM7-(1180–1863) autophosphorylated *in vitro* (see Fig. 1*E* for comparison) indicated that the major phosphorylated sites were included within residues 1180–1863 of TRPM7. The phosphorylation of Ser<sup>1567</sup> in intact cells was confirmed using the phospho-Ser<sup>1567</sup> antibody (Fig. 4*C*). Notably, no phosphorylation of Ser<sup>1567</sup> was found in the inactive TRPM7-TAP mutant. Together, these studies of phosphorylation of TRPM7 *in vitro* and in intact cells indicate that Ser<sup>1511</sup> and Ser<sup>1567</sup> are the major autophosphorylation sites in TRPM7, and at least under basal conditions TRPM7 is not likely to be phosphorylated by other protein kinases in intact cells.

**Characterization of the Role of Autophosphorylation and Kinase Activity of TRPM7 in Regulation of Ca<sup>2+</sup> Influx**—To ex-

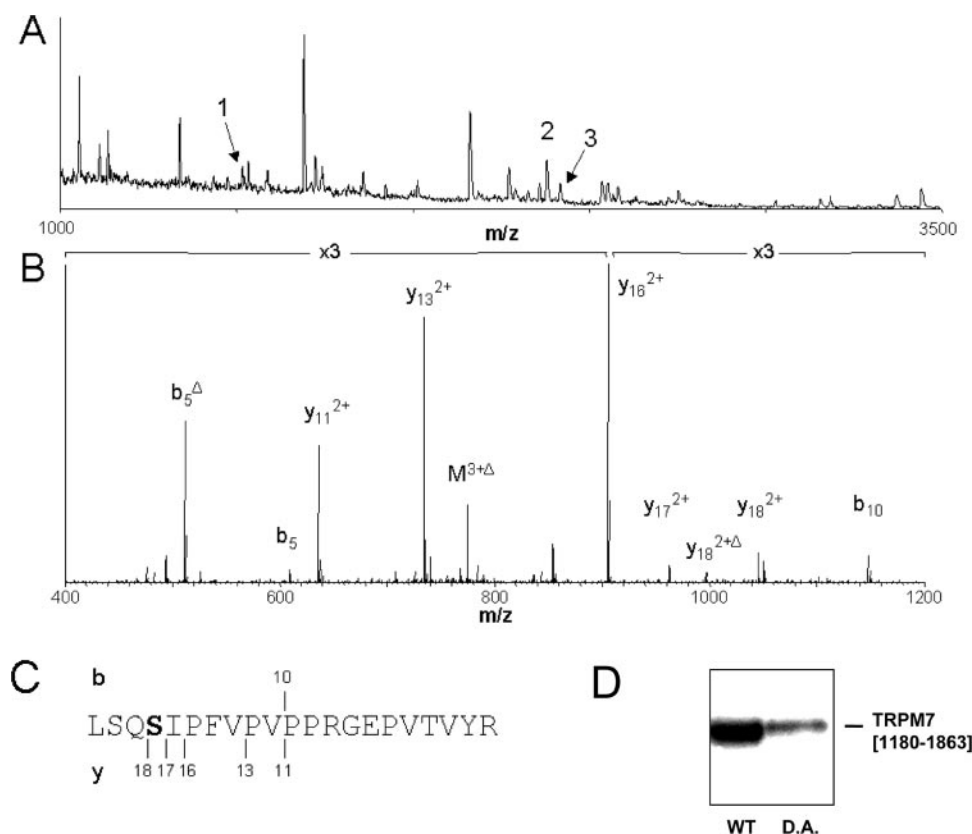


**FIG. 3. Mass spectrometric analysis of autophosphorylation sites in TRPM7.** *A*, GST-TRPM7-(1180–1863) phosphorylated *in vitro* was subjected to SDS-PAGE, in-gel tryptic digestion, and MALDI-TOF mass spectrometry. Three peptides shifted by 80 Da from expected tryptic fragments are indicated: 1, residues 1564–1576; 2, residues 1501–1521; 3, residues 1564–1584. *B*, peptide 3 from *A* was analyzed by HPLC-MS/MS. The fragmentation spectrum of the triply charged ion is shown, and observed b and y ions are labeled. Fragment ions that have lost  $H_3PO_4$  are indicated by  $\Delta$ . *C*, comparison of the fragmentation spectrum with the sequence of the peptide confirms the identity of the peptide and shows that the phosphate in peptide 3 is attached to Ser<sup>1567</sup> (in *boldface type*). *D*, autophosphorylation of GST-TRPM7-(1180–1863) (WT) and mutant GST-TRPM7-(1180–1863) (D.A.) in which Ser<sup>1511</sup> and Ser<sup>1567</sup> were changed to alanine residues. Purified GST fusion proteins were incubated in the presence of [<sup>32</sup>P]MgATP, and the samples were separated by SDS-PAGE and analyzed by autoradiography. <sup>32</sup>P incorporation into the double autophosphorylation (D.A.) site mutant was less than 10% of that of wild type.

amine the effects of the kinase activity of TRPM7 on its functional properties, HEK293 cells were transiently transfected with DNA for wild-type or mutant TRPM7. In initial experiments with wild-type TRPM7 and using an antibody raised against the kinase domain, TRPM7 was found to be expressed in a high percentage of cells (>80%), where it was largely localized in the plasma membrane, although some punctate intracellular immunofluorescence was observed (Fig. 5A). No immunofluorescence was observed in cells transfected with the empty vector. By immunoblotting with an antibody to the coiled-coil domain, full-length TRPM7 was detected as a protein of ~210 kDa, a molecular mass consistent with that predicted from the cDNA sequence (212 kDa) (see Fig. 6A).

To analyze the role of autophosphorylation, Ca<sup>2+</sup> influx through TRPM7 channels was examined in HEK293 cells that expressed either full-length TRPM7 or mutants in which the major autophosphorylation sites, Ser<sup>1511</sup> and Ser<sup>1567</sup>, were mutated to alanine (Fig. 5, *B* and *C*). Cells were initially incubated with Ca<sup>2+</sup>-free buffer (0.5 mM EGTA) and Ca<sup>2+</sup> influx was measured upon addition of 2 mM CaCl<sub>2</sub> to the extracellular medium. No significant Ca<sup>2+</sup> influx was measured in mock-transfected cells (see, for example, Fig. 5D). Comparably large increases in Ca<sup>2+</sup> influx were seen in cells expressing wild-type TRPM7 or autophosphorylation site mutants (S1511A, S1567A, or a S1511A/S1567A double mutant). Moreover, comparably large increases in Ca<sup>2+</sup> influx were observed in cells expressing either wild-type TRPM7 or TRPM7-TAP (Fig. 5D).

We further assessed the potential role of the kinase domain

of TRPM7 by expressing a mutant (TRPM7-(1–1599)) in which most of the kinase domain was deleted (Fig. 6). The expression levels of wild-type TRPM7 and TRPM7-(1–1599) ( $\Delta$ KD) in HEK293 cells were comparable as measured by immunoblotting using an anti-coiled-coil domain antibody (Fig. 6A). In contrast to the full-length kinase-dead TRPM7 (see Fig. 5D), very little Ca<sup>2+</sup> influx was observed in cells expressing TRPM7- $\Delta$ KD (Fig. 6B). A similar result was observed using a different protocol in which cells were incubated initially with Ca<sup>2+</sup>-free buffer (0.5 mM EGTA) and thapsigargin (200 nM) to deplete intracellular stores, and then Ca<sup>2+</sup> influx was measured upon the addition of 2 mM CaCl<sub>2</sub> to the extracellular medium (Fig. 6C).

**Whole-cell Patch Clamp Recordings from CHO Cells Overexpressing Wild-type and Mutant TRPM7 Proteins**—Inclusion of millimolar internal Mg<sup>2+</sup>, MgATP, or MgGTP inhibits the development of TRPM7 current (6). Previous studies have demonstrated that wild-type TRPM7 channel activity can be induced during whole cell recording by lowering internal Mg<sup>2+</sup> by dialysis with pipette solutions lacking Mg<sup>2+</sup> (5, 6). We therefore evaluated channel activity by whole-cell recording using Mg<sup>2+</sup>-free internal solutions in CHO cells that expressed wild-type and mutant TRPM7. A typical *I*-*V* relationship (*top*) and time course for development of the wild-type TRPM7 current is shown (Fig. 7A). Immediately following break-in to achieve whole-cell recording, the current was small but detectable (20-s trace) and increased gradually over the course of several minutes (6-min trace). The autophosphorylation site mutant (Fig.

7, B and E) and the kinase-dead mutant (Fig. 7, C and E) also exhibited currents that developed with *I-V* characteristics and a time course which was the same as wild-type TRPM7. The current immediately after break-in represents activity of pre-activated channels and was variable from cell to cell (shown in Fig. 7E). Moreover, the kinetics of the current development and rundown varied greatly from cell to cell but did not depend on the expressed construct (compare Fig. 7, A–C). In contrast, the TRPM7- $\Delta$ KD mutant failed to express significant channel activity (Fig. 7, D and E). The comparatively small current in untransfected CHO cells is the endogenous MIC current, which is thought to represent native TRPM7 protein (Fig. 7D, and data not shown for mock-transfected cells). Thus, although deletion of the kinase domain abolished TRPM7 channel activity, the endogenous current was unaffected.

We next examined  $Mg^{2+}$  inhibition of wild-type TRPM7 and the various mutants by comparing the extent of inhibition by two concentrations of internal  $Mg^{2+}$  (~2.3 and 4 mM free concentrations) (Fig. 8 and data not shown). Pre-activated current was detected immediately after break-in, and the current subsequently declined over minutes as  $Mg^{2+}$  entered the cell (Fig. 8, A–D, shows representative results for ~2.3 mM free  $Mg^{2+}$ ). No apparent difference was detected between the time courses of  $Mg^{2+}$  inhibition between wild type, the double autophosphorylation site, or the kinase-dead mutant. Normalized current amplitudes at break-in for individual cells are summarized in Fig. 8E. In order to address the extent of  $Mg^{2+}$  inhibition quantitatively, we measured the current amplitude after steady-state inhibition was established (usually ~400 s after break-in) and divided this value by the amplitude at break-in ( $I_0$ ). This approach was chosen because channel expression varied greatly from cell to cell (Fig. 8E), and it allowed us to measure relative  $Mg^{2+}$  inhibition for each cell individually. The extent of  $Mg^{2+}$  inhibition determined in this fashion was not significantly different at either 2.3 or 4 mM  $Mg^{2+}$  for wild-type TRPM7 and the autophosphorylation site or kinase-dead mutants (Fig. 8F).

**Effects of Divalent Cations on the Kinase and Channel Activities of TRPM7**—In further experiments, we compared the effects of divalent ions on both channel and kinase activities of TRPM7. As expected, MBP kinase activity required  $Mg^{2+}$  with maximal activity being observed with a concentration of 10 mM (Fig. 9A). In the presence of 10 mM  $Mg^{2+}$ , the addition of  $Ca^{2+}$  had no effect on kinase activity (Fig. 9A) or autophosphorylation (data not shown). Notably, the addition of  $Ca^{2+}$  plus calmodulin resulted in inhibition of MBP phosphorylation, presumably as a result of binding to the MBP substrate (24). In the presence of 10 mM  $Mg^{2+}$ , the addition of high concentrations of  $Zn^{2+}$  strongly inhibited kinase activity (Fig. 9A) and autophosphorylation (data not shown), presumably by competing with  $Mg^{2+}$ . Similar results were observed in a recent study by Ryazanov *et al.* (24) (see also Schmitz *et al.*, (10)).

We next examined effects of  $Ca^{2+}$  and  $Zn^{2+}$  on TRPM7 current. In a control experiment where the internal solution contained no divalent cations (1 mM EDTA), TRPM7 current increased over time (Fig. 9B). The addition of 5 mM  $CaCl_2$  (Fig. 9C) or 5 mM  $ZnCl_2$  (Fig. 9D) reduced TRPM7 current markedly (note different y axis units). The extent of inhibition was similar to that of  $Mg^{2+}$  (see Fig. 8) in that it was voltage-independent and proceeded with a similar time course. Thus, although  $Mg^{2+}$  is required,  $Ca^{2+}$  has no effect, and  $Zn^{2+}$  inhibits TRPM7 kinase activity, all three cations inhibited TRPM7 channel current.

#### DISCUSSION

**Characterization of TRPM7 Activity and Autophosphorylation**—TRPM7 is unusual in that it is a TRP-like ion channel

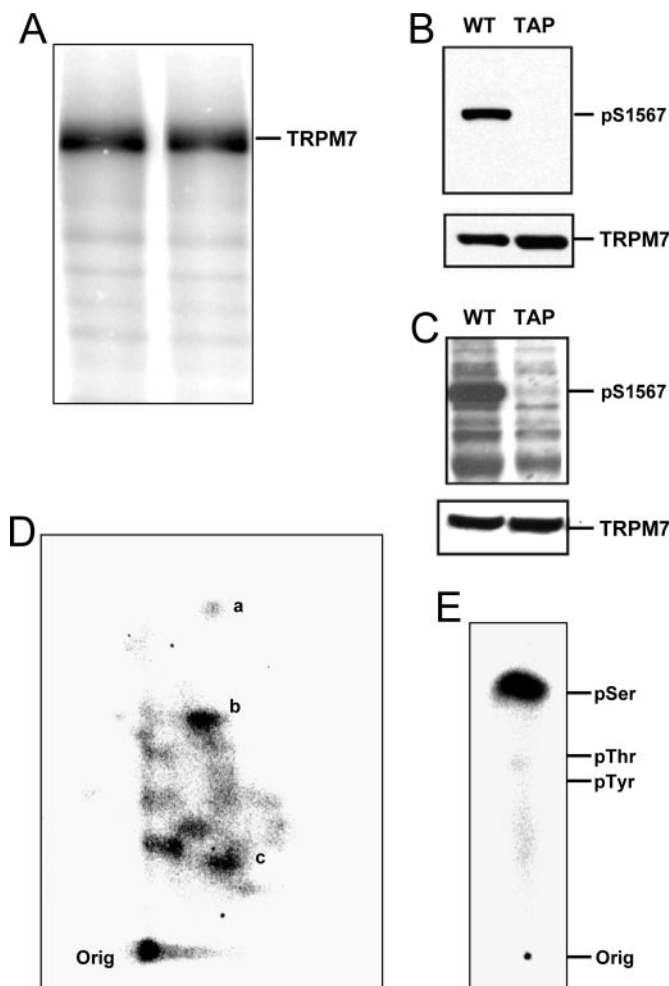


**FIG. 4. Phosphorylation of TRPM7 in intact cells.** A, wild-type TRPM7 was expressed in HEK293 cells, cells were labeled with  $^{32}P_i$  for 2 h, cell lysates were prepared, and TRPM7 was immunoprecipitated. Samples were analyzed by SDS-PAGE and autoradiography. Duplicate samples from separate cultures of cells are shown. B, characterization of phospho-Ser<sup>1567</sup> antibody. Purified wild-type GST-TRPM7 (1180–1863) (WT) or GST-TRPM7-TAP (TAP) were incubated in the presence of MgATP. The samples were separated by SDS-PAGE and analyzed by immunoblotting using the phospho-Ser<sup>1567</sup> (top) or the anti-kinase domain (bottom) antibody. C, phosphorylation of Ser<sup>1567</sup> in intact cells. Wild-type TRPM7-WT (WT) or TRPM7-TAP (TAP) were expressed in HEK293 cells, and TRPM7 was immunoprecipitated with anti-FLAG M2 affinity gel. Samples were separated by SDS-PAGE and analyzed by immunoblotting using the phospho-Ser<sup>1567</sup> (top panel) or anti-FLAG (bottom panel) antibody. D, two-dimensional tryptic phosphopeptide map of TRPM7 phosphorylated in intact cells as shown in A. The samples were separated by electrophoresis in the first dimension (origin left, positive right) and by ascending chromatography in the second dimension. Major phosphopeptides a, b, and c are indicated. See Fig. 1E for comparison with TRPM7 phosphorylated *in vitro*. E, phosphoamino acid analysis of TRPM7 phosphorylated in intact cells as shown in A.

that includes a Ser/Thr protein kinase within a single polypeptide chain. Moreover, the kinase domain of TRPM7 is itself atypical in that it is distinct in structure from the superfamily of eukaryotic protein kinases. Our recent elucidation of its crystal structure suggests that the TRPM7 kinase and other related kinase domains may represent an intermediate stage in the evolution of the protein kinase A-like protein kinases from metabolic enzymes. Notably, some other members of the EF2K/MHCK family of protein kinases are predicted to contain membrane-spanning domains (1, 3). It will be of interest to examine if any of these other atypical kinases are components of ion channels. Despite the absence of any overall amino acid sequence similarity, the results from our site-directed mutagen-

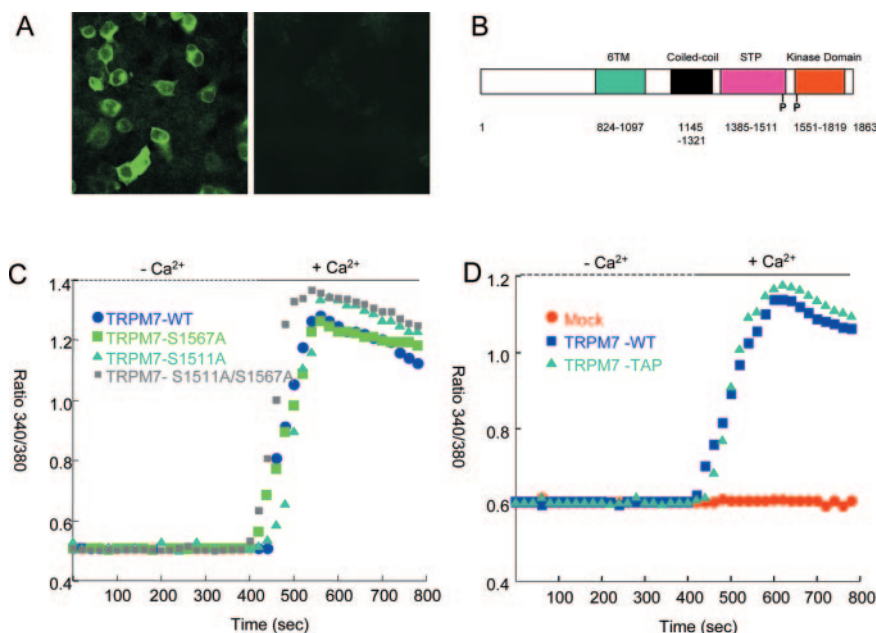


**FIG. 5.  $\text{Ca}^{2+}$  influx in HEK293 cells expressing wild-type, phosphorylation site, and kinase-dead mutants of TRPM7.** A, the expression of TRPM7 was examined in mock-transfected HEK293 cells (right) or in cells expressing full-length wild-type TRPM7 (left), using indirect immunofluorescence with an anti-kinase domain antibody. B, the diagram shows the position of the phosphorylation sites within the domain organization of TRPM7. C, intracellular  $\text{Ca}^{2+}$  levels were measured using FURA-2 in cells expressing wild-type TRPM7 (*TRPM7-WT*) or TRPM7 in which Ser<sup>1511</sup>, Ser<sup>1567</sup>, or both Ser<sup>1511</sup> and Ser<sup>1567</sup> were mutated to alanine. Cells were incubated with  $\text{Ca}^{2+}$  free buffer (0.5 mM EGTA, dashed line at top of graph) and  $\text{Ca}^{2+}$  influx was measured upon the addition of 2 mM  $\text{CaCl}_2$  to the extracellular medium (solid line at top of graph). D, intracellular  $\text{Ca}^{2+}$  levels were measured in mock-transfected cells (*Mock*), cells expressing full-length TRPM7 (*TRPM7-WT*), or TRPM7 in which the kinase activity was inactivated by a mutation of Asp<sup>1775</sup> to alanine in the active site (*TRPM7-TAP*).  $\text{Ca}^{2+}$  influx was measured as described for Fig. 5C.

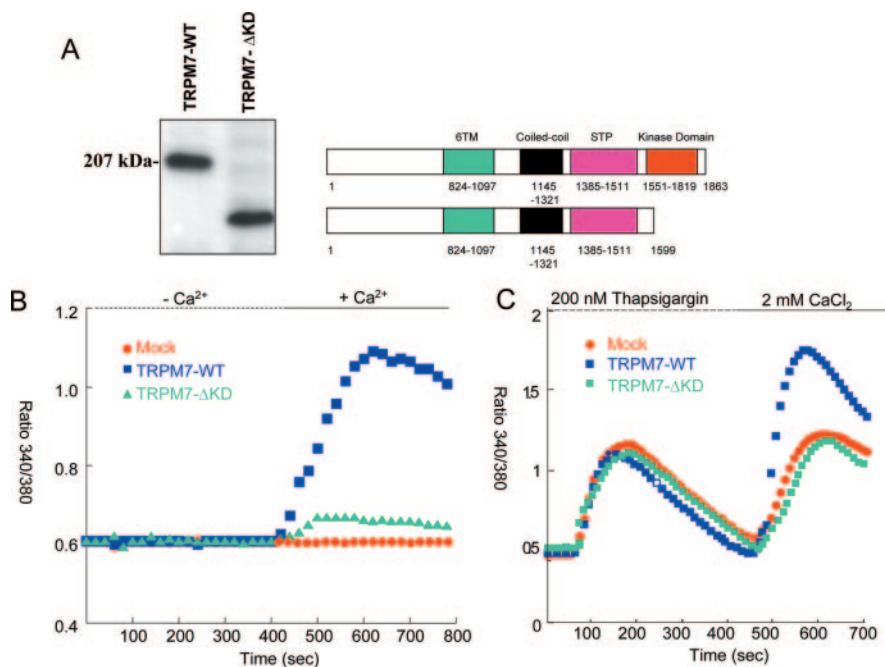


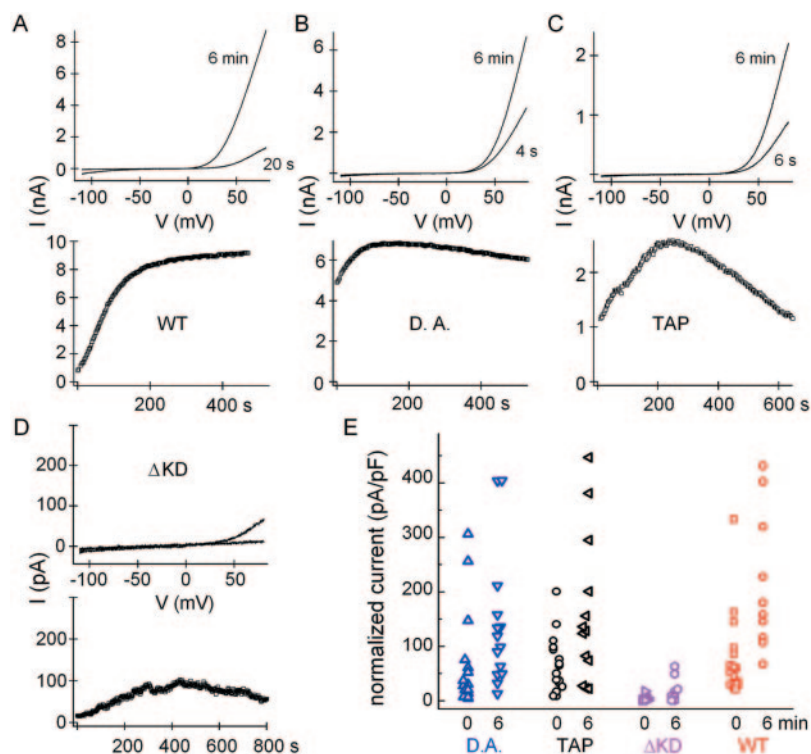
**FIG. 6.  $\text{Ca}^{2+}$  influx in HEK293 cells expressing wild-type TRPM7 or a deletion mutant of TRPM7 lacking the kinase domain.** A, the expression levels of wild-type TRPM7 (*TRPM7-WT*), and a truncated TRPM7 in which the kinase domain was deleted (*TRPM7-ΔKD* and *TRPM7-(1-1599)*), were analyzed by immunoblotting using an anti-coiled-coil domain antibody. The diagram on the right shows the domain organization of TRPM7-WT and TRPM7-ΔKD. B, intracellular  $\text{Ca}^{2+}$  levels were measured using FURA-2 in mock-transfected cells (*Mock*), cells expressing TRPM7-WT, or cells expressing TRPM7-ΔKD. Cells were incubated with  $\text{Ca}^{2+}$ -free buffer (0.5 mM EGTA, dashed line at top of graph), and  $\text{Ca}^{2+}$  influx was measured upon the addition of 2 mM  $\text{CaCl}_2$  to the extracellular medium (solid line at top of graph). C, cells were incubated with  $\text{Ca}^{2+}$ -free buffer (0.5 mM EGTA) and thapsigargin (200 nM) to deplete intracellular stores (dashed line at top of graph).  $\text{Ca}^{2+}$  influx was measured upon the addition of 2 mM  $\text{CaCl}_2$  to the extracellular medium (solid line at top of graph).

esis studies highlight the conservation of function of several key amino acid residues in the active sites of the two classes of protein kinase. Thus, mutation of residues involved directly in binding of phosphate groups of ATP or involved in metal bind-

ing or catalysis resulted in very low kinase activity. For example, mutation of Lys<sup>1646</sup> (to arginine) confirmed this residue as being equivalent to the conserved lysine that is often mutated to produce a “kinase-dead” classical kinase. In addition, muta-

**FIG. 7. Whole-cell patch clamp recordings from CHO cells overexpressing wild-type and mutant TRPM7 proteins.**

Wild-type and mutant forms of TRPM7 were expressed in CHO cells and current recorded in whole-cell patch clamp mode. Current-voltage relations (top panels) and the time course (bottom panels) of development of TRPM7 current are shown for wild type (WT) (A), S1511A/S1567A double autophosphorylation site mutant (D.A.) (B), kinase-dead mutant (TAP) (C), and kinase-domain deletion mutant ( $\Delta$ KD) (D). The top panels in A–D show the current-voltage relation at break-in (4–20 s) and 6 min after cell dialysis with the  $Mg^{2+}$ -free pipette solution. Note that from comparison with results from studies of mock-transfected cells (not shown), only the background endogenous  $Mg^{2+}$ -inhibited cation current is detected in D. E shows the current amplitude at +80 mV normalized to the cell capacitance. 0 and 6 min represent points taken at break-in and 6 min later (wild type,  $n = 14$  and 14;  $\Delta$ KD,  $n = 6$  and 8; D.A.,  $n = 14$  and 14; TAP,  $n = 16$  and 13).



tion of Asp<sup>1775</sup> (a mutation used in our subsequent functional studies) confirmed this residue as being equivalent to Asp<sup>184</sup> of protein kinase A, a key residue involved in binding of the  $Mg^{2+}$  ion that chelates the  $\beta$ - and  $\gamma$ -phosphates of ATP (4).

Based on their sequence similarity to voltage-gated ion channels, TRPs are likely to form tetramers (12). Our x-ray crystallography studies indicate that two kinase domains of TRPM7 associate as a domain-swapped dimer. Thus, a TRPM7 homotetramer would consist of two pairs of dimers, with dimerization probably being restricted to adjacent, but not diagonally opposed, neighbors. Alternatively, dimerization could occur between either adjacent or diagonally opposed TRPM7 monomers in a tetrameric channel formed with one or two other TRP family members. In this regard, TRPM7 appears to be able to interact with the closely related TRPM6, and co-assembly of TRPM6/M7 complexes appears necessary for functional expression of TRPM6 at the plasma membrane (11). In this study, we identified two major phosphorylation sites in TRPM7 at Ser<sup>1511</sup> and Ser<sup>1567</sup>. Ser<sup>1511</sup> is present within a region of TRPM7 of unknown function but that contains numerous Ser/Pro and Thr/Pro motifs. Ser<sup>1567</sup> is located just after the first  $\alpha$  helix ( $\alpha_A$ ) of the kinase domain, the  $\alpha_A$  helix being the main structural element of the segment that is “exchanged” between the two monomers. The autophosphorylation of these sites appears to have no effect on kinase activity (24), but it seems possible that phosphorylation of Ser<sup>1567</sup> in particular has the potential to affect the dimeric structure or stability of the paired kinase domains.

Previous studies have shown that EF2 kinase and MHCK both phosphorylate threonine residues within their respective substrates (25, 26). These results raised the possibility that atypical kinases might be selective for threonine. However, the two autophosphorylation sites identified in this study are serine residues, and serine is the residue that is phosphorylated in MBP. The EF2K/MHCK family of atypical protein kinases are unlikely, therefore, as a group to show preference for threonine in their respective substrates. Moreover, the EF2K/MHCK family kinases do not seem to recognize any obvious consensus

phosphorylation site motif. Ser<sup>1511</sup> and Ser<sup>1567</sup> are found within the amino acid sequences, STEDSPEVDS(P)KAALLP-DWLR and MRLSQS(P)IPFVVPVPPR, respectively (boldface type indicates phosphorylated serines). These sites do not exhibit any similarity to each other or to sites phosphorylated by other EF2K/MHCK family members. Structure-function studies of EF2 kinase and MHCK have suggested that interactions with substrate require additional protein/protein interactions outside of the immediate contacts at the active site. For example, EF2 interacts directly with the extreme C terminus of EF2 kinase, a region removed from the catalytic domain by ~300 amino acids (25, 27, 28). In MHCK-A, the catalytic domain is flanked at the N terminus by a coiled-coil region, and at the C terminus by a 7-fold WD repeat motif. Removal of the WD repeat domain decreased significantly the rate of phosphorylation of full-length myosin but had no effect on the kinetics of phosphorylation of a short synthetic peptide that served as a substrate for the kinase (29). Presumably, these additional targeting interactions stabilize the interaction of EF2 or myosin with their respective kinase and perhaps orient the region containing the phosphorylation sites of EF2 or myosin in the correct position in the active sites of either kinase. Similar secondary interaction domains away from the active site of the kinase may also be required for recognition of substrates for TRPM7.

Our studies indicate that the major sites autophosphorylated *in vitro*, Ser<sup>1511</sup> and Ser<sup>1567</sup>, are also the main sites phosphorylated in intact cells, at least under control conditions. It is possible that upon stimulation, one or more kinases could phosphorylate TRPM7 and regulate kinase or channel function. It is also possible that  $Ca^{2+}$  or other cations that permeate the TRPM7 channel pore could have a local effect on kinase function.

*Does the TRPM7 Kinase Domain Play Any Role in Regulation of Its Channel Function?*—Given the unique incorporation of a kinase domain within the TRPM6 and TRPM7 polypeptides, it might have been expected that the kinase activity would play a significant role in channel gating. However, the results of the

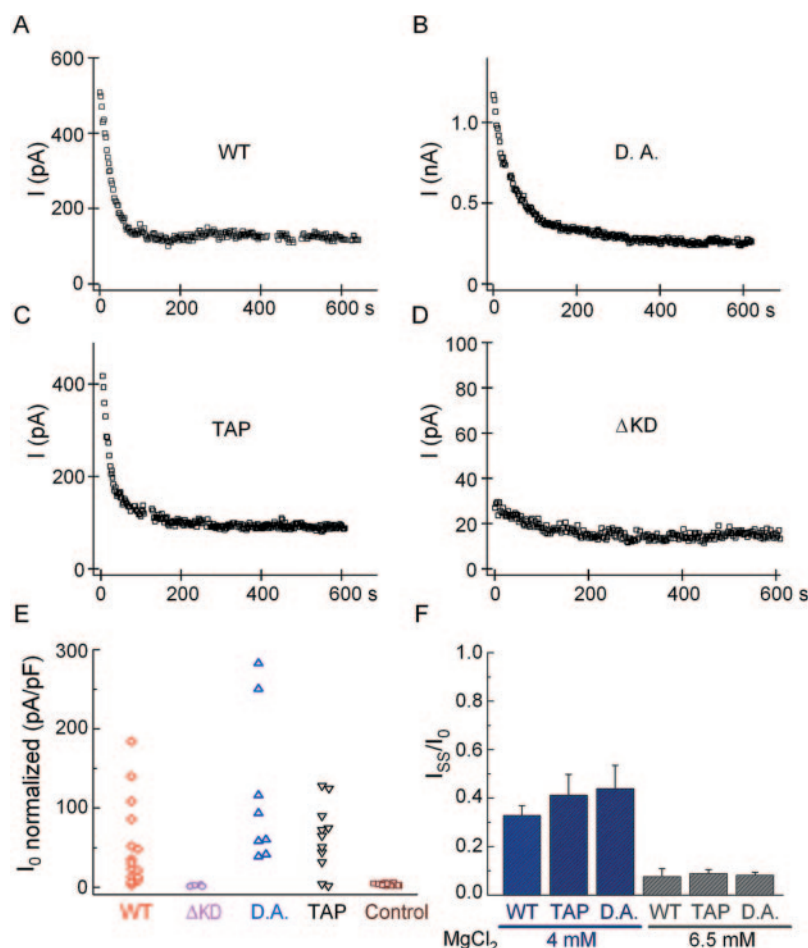


**FIG. 8. Internal Mg<sup>2+</sup> inhibition of TRPM7 currents.** Wild-type and mutant forms of TRPM7 were expressed in CHO cells and current recorded in whole-cell patch clamp mode. Time courses are shown for inhibition of TRPM7 currents by 2.3 mM free internal Mg<sup>2+</sup> (12 mM EGTA plus 4 mM MgCl<sub>2</sub>) for wild type (WT) (A), S1511A/S1567A double autophosphorylation site mutant (D.A.) (B), kinase-dead mutant (TAP) (C), and kinase domain deletion mutant (ΔKD) (D). The current was maximal at break-in ( $t = 0$ ) and declined during subsequent dialysis of the cell interior with the Mg<sup>2+</sup>-containing pipette solution. E, the current amplitudes after break-in (with 12 mM EGTA plus 4 mM MgCl<sub>2</sub>) are shown for untransfected (Control) CHO cells, as well as for cells expressing wild-type and mutant forms of TRPM7 (wild type,  $n = 15$ ; ΔKD,  $n = 5$ ; D.A.,  $n = 8$ ; TAP,  $n = 11$ ; control,  $n = 14$ ). In agreement with the results shown in Fig. 7, wild-type TRPM7, the autophosphorylation site mutant, and kinase-dead mutant all showed amplitudes much greater than the endogenous current, whereas the TRPM7-ΔKD deletion mutant did not exhibit any increase in current compared with control. F, the current amplitude after the establishment of steady state ( $I_{SS}$ ) was divided by the current amplitude at break-in ( $I_0$ ) for each cell examined to determine the percentage inhibition by 2.3 mM (12 mM EGTA plus 4 mM MgCl<sub>2</sub>) and 4 mM (12 mM EGTA plus 6.5 mM MgCl<sub>2</sub>) free Mg<sup>2+</sup>. To minimize contamination by the endogenous MIC current, only cells showing expression levels  $\sim 8$  times the background or higher were selected for this measurement (see E). The normalized current amplitude of untransfected CHO cells at break-in was 4.65 pA/picofarad ( $n = 14$ ). 2.3 mM free Mg<sup>2+</sup> was sufficient to inhibit the endogenous current. Means  $\pm$  S.E. are shown for both internal Mg<sup>2+</sup> concentrations (wild type,  $n = 9$  and 6; TAP,  $n = 7$  and 19; D.A.,  $n = 7$  and 6). The mean current fraction not inhibited by 2.3 mM Mg<sup>2+</sup> was  $0.33 \pm 0.04$  (wild type),  $0.41 \pm 0.08$  (TAP), and  $0.44 \pm 0.095$  (D.A.). The mean current fraction not inhibited by 4 mM Mg<sup>2+</sup> was  $0.07 \pm 0.03$  (wild type),  $0.08 \pm 0.01$  (TAP), and  $0.08 \pm 0.01$  (D.A.).

current study failed to find any obvious regulatory function for the TRPM7 kinase activity. We assessed channel function in several different ways and analyzed the effect of several different types of mutations of TRPM7. Measurement of Ca<sup>2+</sup> influx into intact cells, or by carrying out whole-cell recording with Mg<sup>2+</sup>-free internal solutions, indicated that mutation of the major autophosphorylation sites in TRPM7 or inactivation of kinase catalytic function had no significant effect compared with results obtained with wild-type TRPM7. Our analysis of autophosphorylation site mutants has the added advantage of ruling out the possibility that low levels of endogenous TRPM7 kinase activity might be sufficient to result in significant phosphorylation of exogenous TRPM7 kinase mutants.

Two previous studies have attempted to address the role of the TRPM7 kinase domain in channel function (5, 10). Although these two studies were not in agreement with each other, they concluded that TRPM7 kinase activity was either essential to (5) or was involved in modulating (10) channel

function. Runnels *et al.* (5) mutated Gly<sup>1796</sup> (to aspartate, incorrectly assuming that this residue was part of the ATP binding site) and mutated Cys<sup>1809</sup> and Cys<sup>1812</sup> (to alanine, incorrectly assuming that these residues were part of a "FYVE" zinc finger motif) and were not able to measure whole-cell currents in these mutants. Unfortunately, no positive controls were provided to show that the mutant TRPM7 channels were actually expressed. Subsequently, Schmitz *et al.* (10) showed that mutation of Gly<sup>1799</sup> (to aspartate) (a residue equivalent to the Gly<sup>1796</sup> studied by Runnels *et al.* (5)) or mutation of Lys<sup>1648</sup> (to arginine; same as one of the mutants studied here) resulted in active channels. Our results are in general agreement with the findings of Schmitz *et al.* (10) concerning the lack of any essential role for TRPM7 kinase activity in the control of channel function. It seems likely, therefore, that the results obtained by Runnels *et al.* (5) reflected a failure of TRPM7 mutant protein expression or trafficking.

Schmitz *et al.* (10) also examined the sensitivity of kinase

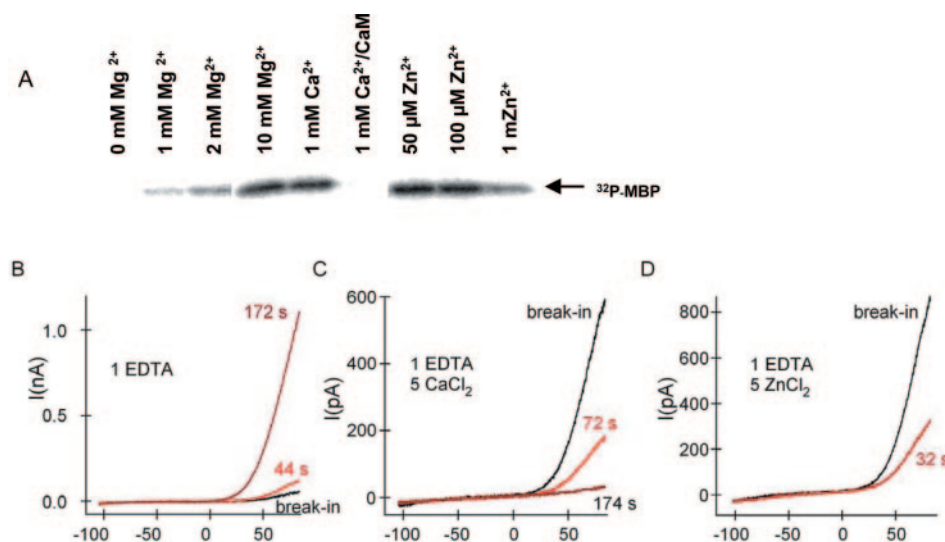


FIG. 9. **Effects of divalent cations on kinase and channel activities of TRPM7.** A, MBP was incubated with GST-TRPM7-(1180–1863) in the presence of various concentration of divalent cations or CaM and as indicated, with the samples containing  $\text{Ca}^{2+}$  or  $\text{Zn}^{2+}$  also including 10 mM  $\text{Mg}^{2+}$ . Samples were incubated with [ $^{32}\text{P}$ ]ATP for 10 min and then separated by SDS-PAGE and analyzed using a phosphor imager. B, wild-type TRPM7 current development in 1 mM EDTA solution. I-V plots were obtained at the indicated times after break-in. C, inhibition of preactivated TRPM7 current by 5 mM  $\text{CaCl}_2$  plus 1 mM EDTA. D, inhibition of preactivated TRPM7 current by 5 mM  $\text{ZnCl}_2$  plus 1 mM EDTA. The x axis in panels B and C represents voltage, v(mV).

mutant channels to internal  $\text{Mg}^{2+}$  and showed that at lower concentrations ( $\sim 3$  mM)  $\text{Mg}^{2+}$ , inhibition was reduced for the two kinase domain mutants, whereas at higher concentrations (7–8 mM), inhibition was identical to the wild-type channel. This differs from our results indicating that TRPM7 kinase activity had no effect on  $\text{Mg}^{2+}$  inhibition. The reason for this discrepancy is unknown at present. It is worth mentioning, however, that Schmitz *et al.* (10) measured averages of current amplitudes for groups of cells, whereas we compared TRPM7 inhibition in individual cells and averaged those. It is possible that variability of channel expression influenced the analysis of Schmitz *et al.* (10).

A significant result from our current studies is that deletion of the entire kinase domain of TRPM7 resulted in production of an apparently inactive channel as measured by  $\text{Ca}^{2+}$  influx or from whole-cell recording methods. The level of expression of the truncated TRPM7- $\Delta\text{KD}$  deletion mutant was similar to that of wild-type TRPM7. However, we cannot rule out the possibility that the protein was not normally assembled as a tetramer and/or processed and trafficked to the plasma membrane. Schmitz *et al.* (10) also examined the properties of a slightly shorter TRPM7- $\Delta\text{KD}$  deletion mutant (residues 1–1569). Whole-cell recordings indicated that cells expressing the 1–1569 TRPM7- $\Delta\text{KD}$  deletion mutant exhibited significantly reduced TRPM7 currents ( $\sim 10\%$  of that of cells expressing wild-type TRPM7) perhaps reflecting different properties of the mutant used or of its expression level. Schmitz *et al.* (10) also suggested that their TRPM7- $\Delta\text{KD}$  deletion mutant was much more sensitive to inhibition by  $\text{Mg}^{2+}$ . However, given the much reduced currents, it is difficult to derive clear conclusions from the data shown.

We also examined the regulation of channel function and kinase activity by different divalent cations. The results from measurement of kinase activity *in vitro* indicated that while  $\text{Mg}^{2+}$  is required for kinase activity,  $\text{Ca}^{2+}$  has no effect, and  $\text{Zn}^{2+}$  inhibits kinase activity. These results are in complete agreement with a recent study by Ryazanova *et al.* (24). However, in circumstantial support of the conclusion that kinase activity is dissociated from channel function, these three cations inhibited TRPM7 channel current (see also Ref. 30). Additional circumstantial evidence for lack of role of kinase activ-

ity in regulation of channel function comes from consideration of the fact that both MgATP and MgGTP inhibit channel activity (6), whereas only MgATP is capable of supporting TRPM7 kinase activity (24).

#### CONCLUSIONS

Together, our results demonstrate that TRPM7 channel activity and sensitivity to inhibition by divalent cations are dissociated from the activity of the intrinsic kinase domain. The function of the kinase domain is therefore unknown at the present time. Presumably, other substrates for TRPM7 kinase exist, and these may be involved in signal transduction pathways somehow linked to channel activity. The kinase domain of TRPM7 is known to interact with various phospholipase C isoforms, although the functional significance of these interactions is not known (17). TRPM7 kinase activity or autophosphorylation may influence the interaction with phospholipase C or with other unidentified proteins. The results from our current study indicate that whereas kinase activity is not essential for channel function, the presence of the kinase domain is critical for functional expression of TRPM7. Future studies will hopefully clarify the role(s) that this unusual kinase domain plays in the expression and regulation of TRPM7.

#### REFERENCES

- Ryazanova, A. G. (2002) *FEBS Lett.* **514**, 26–29
- Nairn, A. C. (2003) *Atypical Protein Kinases: The EF2K/MHCK/ChaK Kinase Family*, pp. 567–573, Academic Press, New York
- Drennan, D., and Ryazanova, A. G. (2004) *Prog. Biophys. Mol. Biol.* **85**, 1–32
- Yamaguchi, H., Matsushita, M., Nairn, A. C., and Kuriyan, J. (2001) *Mol. Cell* **7**, 1047–1057
- Runnels, L. W., Yue, L., and Clapham, D. E. (2001) *Science* **291**, 1043–1047
- Nadler, M. J., Hermosura, M. C., Inabe, K., Perraud, A. L., Zhu, Q., Stokes, A. J., Kurosaki, T., Kinet, J. P., Penner, R., Scharenberg, A. M., and Fleig, A. (2001) *Nature* **411**, 590–595
- Clapham, D. E., Montell, C., Schultz, G., and Julius, D. (2003) *Pharmacol. Rev.* **55**, 591–596
- Schlingmann, K. P., Weber, S., Peters, M., Niemann, N. L., Vitzthum, H., Klingel, K., Kratz, M., Haddad, E., Ristoff, E., Dinour, D., Syrrou, M., Nielsen, S., Sassen, M., Waldegger, S., Seyberth, H. W., and Konrad, M. (2002) *Nat. Genet.* **31**, 166–170
- Walder, R. Y., Landau, D., Meyer, P., Shalev, H., Tsolia, M., Borochowitz, Z., Boettger, M. B., Beck, G. E., Englehardt, R. K., Carmi, R., and Sheffield, V. C. (2002) *Nat. Genet.* **31**, 171–174
- Schmitz, C., Perraud, A. L., Johnson, C. O., Inabe, K., Smith, M. K., Penner, R., Kurosaki, T., Fleig, A., and Scharenberg, A. M. (2003) *Cell* **114**, 191–200
- Chubanov, V., Waldegger, S., Schnitzler, M., Vitzthum, H., Sassen, M. C., Seyberth, H. W., Konrad, M., and Gudermann, T. (2004) *Proc. Natl. Acad.*

- Sci. U. S. A.* **101**, 2894–2899
12. Harteneck, C., Plant, T. D., and Schultz, G. (2000) *Trends Neurosci.* **23**, 159–166
  13. Montell, C. (2001) *Sci. STKE* 2001, RE1, 1–17
  14. Hermosura, M. C., Monteilh-Zoller, M. K., Scharenberg, A. M., Penner, R., and Fleig, A. (2002) *J. Physiol. (Lond.)* **539**, 445–458
  15. Prakriya, M., and Lewis, R. S. (2002) *J. Gen. Physiol.* **119**, 487–507
  16. Kozak, J. A., Kerschbaum, H. H., and Cahalan, M. D. (2002) *J. Gen. Physiol.* **120**, 221–235
  17. Runnels, L. W., Yue, L., and Clapham, D. E. (2002) *Nat. Cell Biol.* **4**, 329–336
  18. Zakharov, S. I., Smani, T., Leno, E., Macianskiene, R., Mubagwa, K., and Bolotina, V. M. (2003) *Br. J. Pharmacol.* **138**, 234–244
  19. Jiang, X., Newell, E. W., and Schlichter, L. C. (2003) *J. Biol. Chem.* **278**, 42867–42876
  20. Fleig, A., and Penner, R. (2004) *Trends Pharmacol. Sci.* **25**, 633–639
  21. Nairn, A. C., and Greengard, P. (1987) *J. Biol. Chem.* **262**, 7273–7281
  22. Krutchinsky, A. N., Kalkum, M., and Chait, B. T. (2001) *Anal. Chem.* **73**, 5066–5077
  23. Chalfie, M., Tu, Y., Euskirchen, G., Ward, W. W., and Prasher, D. C. (1994) *Science* **263**, 802–805
  24. Ryazanova, L. V., Dorovkov, M. V., Ansari, A., and Ryazanov, A. G. (2004) *J. Biol. Chem.* **279**, 3708–3716
  25. Pavur, K. S., Petrov, A. N., and Ryazanov, A. G. (2000) *Biochemistry* **39**, 12216–12224
  26. Luo, X., Crawley, S. W., Steimle, P. A., Egelhoff, T. T., and Cote, G. P. (2001) *J. Biol. Chem.* **276**, 17836–17843
  27. Diggle, T. A., Sehra, C. K., Hase, S., and Redpath, N. T. (1999) *FEBS Lett.* **457**, 189–192
  28. Nairn, A. C., Matsushita, M., Nastiuk, K., Horiuchi, A., Mitsui, K., Shimizu, Y., and Palfrey, H. C. (2001) *Prog. Mol. Subcell. Biol.* **27**, 91–129
  29. Kolman, M. F., and Egelhoff, T. T. (1997) *J. Biol. Chem.* **272**, 16904–16910
  30. Kozak, J. A., and Cahalan, M. D. (2003) *Biophys. J.* **84**, 922–927